HHS Public Access

Author manuscript

Free Radic Biol Med. Author manuscript; available in PMC 2016 October 01.

Published in final edited form as:

Free Radic Biol Med. 2015 October ; 87: 36–47. doi:10.1016/j.freeradbiomed.2015.05.042.

Targeting mitochondrial reactive oxygen species to modulate hypoxia-induced pulmonary hypertension

Sherry E. Adesina, **Bum-Yong Kang**, **Kaiser M. Bijli**, **Jing Ma**, **Juan Cheng**, **Tamara Murphy**, **C. Michael Hart**, and **Roy L. Sutliff***

Division of Pulmonary, Allergy, and Critical Care Medicine, Department of Medicine, Atlanta Veterans Affairs and Emory University Medical Centers, Atlanta, GA 30033

Abstract

Objective—Pulmonary hypertension (PH) is characterized by increased pulmonary vascular remodeling, resistance, and pressures. Reactive oxygen species (ROS) contribute to PH-associated vascular dysfunction. NADPH oxidases (Nox) and mitochondria are major sources of superoxide ($O_2^{\bullet-}$) and hydrogen peroxide (H_2O_2) in pulmonary vascular cells. Hypoxia, a common stimulus of PH, increases Nox expression and mitochondrial ROS (mtROS) production. The interactions between these two sources of ROS generation continue to be defined. We hypothesized that mitochondria-derived $O_2^{\bullet-}$ ($mtO_2^{\bullet-}$) and H_2O_2 (mtH_2O_2) increases Nox expression to promote PH pathogenesis and that mitochondria-targeted antioxidants can reduce mtROS, Nox expression, and hypoxia-induced PH.

Approach and Results—Exposure of human pulmonary artery endothelial cells to hypoxia for 72 hours increased $mtO_2^{\bullet-}$ and mtH_2O_2. To assess the contribution of $mtO_2^{\bullet-}$ and mtH_2O_2 to hypoxia-induced PH, mice that overexpress superoxide dismutase 2 (Tg^{hSOD2}) or mitochondria-targeted catalase (MCAT) were exposed to normoxia (21% O_2) or hypoxia (10% O_2) for 3 weeks. Compared to hypoxic control mice, MCAT mice developed less hypoxia-induced increases in RVSP, α-SMA staining, extracellular H_2O_2 (Amplex Red), Nox2 and Nox4 (qRT-PCR and western blot), or cyclinD1 and PCNA (western blot). In contrast, Tg^{hSOD2} mice experienced exacerbated responses to hypoxia.

Conclusions—These studies demonstrate that hypoxia increases $mtO_2^{\bullet-}$ and mtH_2O_2. Targeting mtH_2O_2 attenuates PH pathogenesis, whereas, targeting $mtO_2^{\bullet-}$ exacerbates PH. These differences in PH pathogenesis were mirrored by RVSP, vessel muscularization, levels of Nox2 and Nox4, proliferation, and H_2O_2 release. These studies suggest that targeted reductions in mtH_2O_2 generation may be particularly effective at preventing hypoxia-induced PH.

Graphical abstract

Address correspondence to: Roy L. Sutliff, PhD, Associate Professor of Medicine, Division of Pulmonary and Critical Care Medicine, Atlanta VAMC (151-P), 1670 Clairmont Road, Decatur, GA 30033, Phone: (404) 321 - 6111 ext. 7053, Fax: 404 - 728 - 7750, rsutlif@emory.edu.

DISCLOSURES

The authors have declared that no competing interests exist.

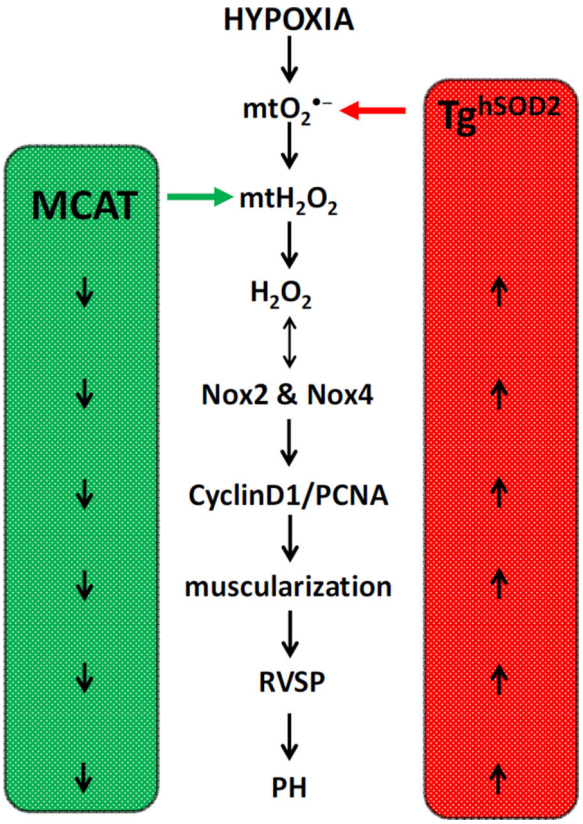

Keywords

Mitochondria; ROS; Hydrogen Peroxide; Superoxide; Catalase; SOD2; NADPH Oxidase; Pulmonary Hypertension

INTRODUCTION

Pulmonary hypertension (PH) is characterized by vasoconstriction and proliferation of pulmonary endothelial and smooth muscle cells, increased pulmonary vascular resistance, and right ventricular hypertrophy that can progress to right heart failure and death [1]. Vascular derangements are triggered by diverse stimuli that promote pulmonary endothelial dysfunction [2]. Current evidence suggests that reactive oxygen species (ROS) such as superoxide ($O_2^{\bullet-}$) and hydrogen peroxide (H_2O_2) generated by mitochondria, NADPH oxidases (Noxes), and other enzymatic sources contribute to PH pathogenesis by altering vascular cell proliferation[3–6]. Although hypoxia contributes to mitochondrial dysfunction, the role of different ROS and mechanisms by which mitochondria-derived ROS (mtROS) promote the development of PH continue to be defined [7–10].[1]

Hypoxia causes pulmonary vasoconstriction through complex mechanisms that involve increased intracellular ROS generation [11]. Noxes, important sources of ROS within the vascular wall [12, 13], regulate endothelial function, vascular tone, vascular cell hypertrophy, and apoptosis [14, 15]. ROS derived from Nox isoforms, in particular Nox2

and Nox4, are involved in long-term responses of the pulmonary vasculature to hypoxia [16–18]. Nox2 is expressed in vascular smooth muscle and endothelial cells [19, 20]. Knockout of $gp91^{phox}$ (Nox2) prevented hypoxia-induced $O_2^{\bullet-}$ production and other pathological alterations associated with hypoxia-induced PAH, including: mean right ventricular pressure, medial wall thickening of small pulmonary arteries, and right heart hypertrophy [21, 22]. Unlike Nox2, Nox4 is a constitutively active isoform responsible for basal H_2O_2 production in the vasculature [12, 23–25]. Nox4 expression is increased in murine models of hypoxia-induced PH, in the pulmonary vasculature of PH patients [17, 26, 27], and in pulmonary artery endothelial cells isolated from patients with idiopathic pulmonary arterial hypertension (IPAH) [28]. Pharmacological approaches to inhibit Nox4 [28] or prevent its upregulation during chronic hypoxia [27] attenuated PH. Taken together, these reports indicate that strategies that attenuate Nox upregulation during PH pathogenesis may provide novel therapeutic opportunities in PH.

Mitochondria, another source of vascular ROS, have been viewed both as a target of Nox-derived ROS and as a source of ROS that stimulates Nox activity [15, 29]. mtROS levels depend on the rate of O_2 reduction to superoxide ($O_2^{\bullet-}$) and on the activity of mitochondrial antioxidant mechanisms [30]. Increasing evidence indicates that mtROS contribute to endothelial cell dysfunction[31, 32] and alter redox-signaling pathways that modulate vascular tone [33–35] by activating redox-sensitive transcription factors that stimulate Nox expression [15]. Since mitochondrial dysfunction is associated with increased Nox4 expression [25], and mtROS have been shown to stimulate the activity of Noxes [15], we hypothesized that mtROS may stimulate increases in Nox activity in the lung during PH pathogenesis.

Based on evidence that ROS derived from mitochondria may stimulate Nox activity and that Nox-derived ROS may stimulate mtROS production [36], we sought to further explore interactions between mitochondria- and Nox-derived ROS under hypoxic conditions that are recognized to promote PH *in vivo*. To explore these interactions we employed several mouse models to experimentally manipulate mitochondrial antioxidants. For example, expression and activity of mitochondrial superoxide dismutase 2 (SOD2), which converts $O_2^{\bullet-}$ to H_2O_2, are decreased in human pulmonary artery smooth muscle cells (HPASMCs) exposed to chronic hypoxia, and SOD2 overexpression in HPASMCs reversed the proliferative

---

[1] c-Nox4(−/−): Nox4 knockout mice
$gp91^{phox-/-}$: Nox 2 knockout mice
HPAEC: Human Pulmonary Arterial Endothelial Cells
H_2O_2: hydrogen peroxide
MCAT: transgenic mice with human catalase targeted to mitochondria
mtH_2O_2: mitochondria- derived hydrogen peroxide
mtROS: Mitochondria- derived ROS
$mtO_2^{\bullet-}$: mitochondria-derived superoxide
MCT: monocrotaline
Nox2: NADPH Oxidase 2
Nox4: NADPH Oxidase 4
$O_2^{\bullet-}$: superoxide
PH: pulmonary hypertension
ROS: reactive oxygen species
RVH: right ventricular hypertrophy
RVSPs: right ventricular systolic pressures
Tg^{hSOD2}: transgenic mice with human superoxide dismutase-2 targeted to mitochondria

phenotype seen in PH [37]. Additionally, overexpression of human SOD2 in mice (Tg^{hSOD2}) attenuated Ang-II-induced hypertension and decreased vascular oxidative stress [15]. Another important intracellular antioxidant, catalase, is normally expressed in peroxisomes and converts H_2O_2 to O_2 and water. Exogenous application of PEG-catalase decreased cyclinD1 expression in lung tissue in an animal model of persistent PH of the newborn (PPHN) [38] and prevented hypoxia-induced Nox4 expression [39]. To reduce mitochondrial $O_2^{\bullet-}$ levels, we utilized transgenic mice with overexpression of the human SOD2 transgene [15, 40] and to reduce mitochondrial H_2O_2 we employed mice with mitochondrialtargeted catalase overexpression [41].

The present study tests the hypothesis that mitochondria-derived $O_2^{\bullet-}$ and H_2O_2 regulate Nox expression which promotes PH pathogenesis. Targeting hypoxia-induced mtROS can prevent PH by attenuating mtROS-induced Nox expression and downstream signaling. The current study demonstrates that exposing HPAECs to chronic hypoxia increases mitochondria-derived $O_2^{\bullet-}$ and H_2O_2. Tg^{hSOD2} and MCAT transgenic mouse models are used to discern if targeting mtROS attenuates hypoxia-induced PH, Nox expression, and proliferative markers. Our results establish that mitochondria-derived $O_2^{\bullet-}$ ($mtO_2^{\bullet-}$), mitochondria-derived H_2O_2 (mtH_2O_2), and Nox expression are increased under hypoxic conditions and that PH, Nox expression, and markers of pulmonary vascular cell proliferation are increased by SOD2 overexpression but decreased by targeted overexpression of catalase in mitochondria. These findings describe a novel role for mtH_2O_2 in hypoxia-induced PH pathogenesis and suggest that targeting mtH_2O_2 may represent a novel therapeutic strategy in PH.

MATERIALS AND METHODS

Cell Culture

Human pulmonary arterial endothelial cells (HPAECs) (Clonetics, San Diego, CA) were cultured at 37°C in 5% CO_2 in endothelial cell growth medium (EGM, Lonza, Walkersville, MD) supplemented with 10% fetal bovine serum (FBS), 10 ng/ml human epidermal growth factor, 1 μg/ml hydrocortisone, 50 μg/ml gentamicin, 50 ng/ml amphotericin-B and 12 μg/ml bovine brain extract as we have described previously (25). To assess the effects hypoxia on HPAEC mtROS generation, cells were incubated at 37°C under either normoxic conditions (21% O_2, 5% CO_2) or hypoxic conditions (1% O_2, 5% CO_2) for 72 hours (25).

Confocal Microscopy

In selected studies, HPAECs were cultured on microscope slides and exposed to normoxia or hypoxia for 72 hours. Selected HPAECs were treated with MitoTEMPO (100 nM) daily or PEG-Catalase (1000 U/mL) for the last 24 hours. Cells were incubated at 37°C with DAPI (1.5 μM, Molecular Probes), MitoTracker Red (1 μM, Molecular Probes), Mitotracker Green, (1 μM, Molecular Probes), MitoSOX (10 μM, Invitrogen), or MitoPy1 (10 μM, Tocris) in Krebs Ringer's phosphate glucose (KRPG) buffer for 20–30 minutes in the dark. Cells were washed with KRPG and stored in PBS until ready for microscopy. Using an Olympus BX51 60× water immersion lens, HPAECs were examined and photographed at 1.5×. Using Fluoview analysis program, individual cells were outlined and the intensity of

MitoPY1 or MitoSOX fluorescence were averaged. 50 – 100 cells were counted in 4 different HPAEC cell lines.

Transgenic mouse models

Transgenic mouse models overexpressing SOD2 or expressing mitochondria-targeted catalase were employed in the current study. MCAT mice were provided by Dr. Peter Rabinovitch (University of Washington). To create the MCAT transgene, the carboxy-terminal amino acids, the peroxisomal localization sequence, and initiating methionine of the human catalase gene were deleted from the human catalase gene. An ornithine transcarbamylase leader sequence was added to the amino terminus to target catalase expression to mitochondria. The catalase cDNA was driven by the CMV enhancer element and chicken β–actin promoter. The MCAT mice were generated by microinjection techniques into B6 (B6C3/F1) embryos. After 8 backcrosses, line purity was confirmed. (Charles River Laboratories, Wilmington, MA) (50). Tg^{hSOD2} mice were generated using a transgenic construct containing the human, superoxide dismutase 2 driven by the human β-actin promoter [40]. All littermate controls are homozygous for wildtype genotype. Both MCAT and Tg^{hSOD2} transgenes were ubiquitously expressed with expression levels varying in different tissues [15, 40, 41]. Neither transgenic mouse model displayed an overt phenotype at baseline. All animal studies were reviewed and approved by the Atlanta VA IACUC.

In Vivo hypoxia exposure and assessment of pulmonary hypertension

Litter mate controls, Tg^{hSOD2}, or MCAT mice, ages 6–9 weeks, were utilized for these studies. To assess the effects of transgene overexpression on PH pathogenesis, mice were either housed in ambient air (normoxia, 21% O_2) or hypoxic conditions (10% O_2) for three weeks as we have described (25,42). Right ventricular systolic pressures (RVSP) were assessed using a 0.8 F micro-tip pressure transducer (Scisense, London, Ontario). Mice were anesthetized with isoflurane and a micro-tip pressure transducer was inserted into the right jugular vein and advanced to the right ventricle. Right ventricular pressure was continuously monitored for 10 minutes, and data were analyzed using the Powerlab system (AD Instruments, Denver, CO) (42). Right ventricular hypertrophy was assessed by calculating right ventricle/left ventricle + septum weight ratios (Fulton Index). Mouse hearts were removed and the right ventricle was dissected from the left ventricle and septum. A ratio of the weights of the right ventricle to the left ventricle and septum was determined. To further assess the temporal onset of PH in our model during hypoxia, transthoracic echocardiograms (TTEs) were performed on mice using a Vevo 770 High-Resolution In Vivo Imaging System (VisualSonics, Toronto, ON, Canada) equipped with a RMV 707B High-Frame-Rate Scanhead (frequency band 15– 45 MHz) as described previously (43). During echocardiography, the animals were lightly anesthetized with 1% isoflurane, and the body temperature was continuously monitored using a rectal thermometer probe to maintain body temperature at 36 – 37°C. Under these conditions, heart rates were greater than 400 beats per minute. Two-dimensional and M-mode echocardiography was used to assess wall motion, chamber dimensions, and wall thickness and to calculate fractional shortening.

Immunohistochemical and morphometric analyses were performed to assess pulmonary vascular remodeling (25, 47). Lungs were perfused blood-free, then placed in formalin overnight. Lung tissue was then paraffin embedded. Lung sections (5 μm) were fixed in 4% formaldehyde, washed three times in PBS, and endogenous peroxidase activity was quenched with 3% H_2O_2 in PBS. Sections were permeabilized with 0.05% Tween-20 (PBS-T), blocked with 5% donkey serum and incubated overnight at 4°C with rabbit anti– α-smooth muscle actin (α-SMA) antibody (LabVision Corporation, Fremont, CA) or PCNA antibody (Santa Cruz, sc-7907). Sections were incubated with biotinylated donkey anti-rabbit secondary antibody (Jackson Immunoresearch Laboratories, West Grove, PA) followed by horseradish peroxidase–streptavidin (Vectastain kit, Vector Laboratories, Burlingame, CA) as previously reported (25,42). 10 – 20 arterioles per sample, less than 100 μm in size, were assessed for muscularization and proliferation.

Mitochondrial isolation

Saline perfused cardiac and pulmonary tissues were processed for mitochondrial isolation using a mitochondria isolation kit (Thermo Scientific 89801). Briefly, the tissues were disrupted by manual cutting and dounce homogenization. Samples were then incubated according to the manufacturer's protocol and centrifuged to isolate cytosolic and mitochondrial fractions. Mitochondrial fractions were washed and suspended in mitochondria lysis buffer (2% CHAPS in Tris Buffered Saline) and then subjected to western blot analysis of human catalase levels.

PCR and Western Blotting

Quantitative real-time PCR was employed to measure mRNA levels of catalase, SOD2, Nox2, Nox4, cyclinD1, and proliferating cell nuclear antigen (PCNA) in HPAECs and lung tissue homogenates. Total RNA was isolated from lung tissue with Trizol according to the manufacturer's protocol (Invitrogen, Carlsbad, CA) and reverse transcribed to synthesize cDNA using the iScript cDNA Synthesis Kit (Bio-Rad, Hercules, CA). Target cDNA was amplified using SYBR Green (Applied Biosystems, Hercules, CA). All data were normalized to GAPDH or 9S content of the same sample as previously described (25).

Protein levels of catalase, SOD2, Nox2, Nox4, CyclinD1, PCNA, GAPDH, and β-actin were assessed with Western blotting. HPAECs and tissues were homogenized in buffer (20 mM Tris pH 7.4, 2.5 mM EDTA, 1% Triton X-100, 1% deoxycholic acid, 1% SDS, 100 mM NaCl, 10 mM NaF, 1 mM Na3VO4), centrifuged, and supernatants were collected for determination of protein concentration by bicinchoninic acid (BCA) assay (BioRad). Proteins (30 μg) were loaded in 10% Bis-Tris gels (Invitrogen, Carlsbad, CA), then transferred onto a nitrocellulose membrane (Millipore, Billerica, MA). Nitrocellulose membranes were probed with rabbit anti-catalase (Athens Research & Technology), rabbit anti-Nox4 (Abcam), mouse anti-gp91phox/Nox2 (BD Transduction Laboratories and Santa Cruz), rabbit anti-CyclinD1 (Santa Cruz), mouse anti-PCNA (BD Transduction Laboratories), or mouse anti-Cytochrome C (BD Pharmingen). β-Actin and GAPDH (Santa Cruz) were used as protein loading controls. After washing, membranes were incubated with horseradish peroxidase-conjugated secondary antibody (Jackson ImmunoResearch

Laboratories, Inc., West Grove, PA). Immunodetection was performed using a UV method (LiCor).

Measurement of ROS levels

H_2O_2 was measured by detecting horseradish peroxidase-catalyzed oxidation of the non-fluorescent molecule N-acetyl-3,7-dihydroxyphenoxazine (Amplex Red; Invitrogen) into the highly fluorescent molecule resorufin. Lung tissue was pre-incubated with Krebs Ringer's Phosphate Glucose (KRPG) buffer for 1 hour. Samples were then incubated in KRPG buffer containing 100 μl/ml Amplex Red and 0.2 U/ml Horseradish peroxidase (HRP) for 1 hour at 37°C. Menadione (0.5 M) was used as positive control or 1000U/mL PEG-Catalase was used as negative control to assess H_2O_2 production. Resorufin fluorescence was measured with a Wallac fluorimeter (PerkinElmer, Waltham, MA) at excitation and emission wavelengths of 540 nm and 590 nm, respectively. Sample fluorescence was compared to that generated by a H_2O_2 standard curve to calculate the concentrations of H_2O_2 released from tissue. H_2O_2 concentrations were normalized to tissue wet weight (71).

Statistical Analysis

For all experiments, data were analyzed using Student's t-test for studies with two groups. For studies with three or more groups two - way analysis of variance (ANOVA) followed by post-hoc analysis with the Tukey test to detect differences between individual groups. A value of $p < 0.05$ was considered statistically significant for all statistical analyses (42, 71).

RESULTS

Hypoxia increases mitochondrial ROS generation in HPAECs

HPAECs were cultured under either normoxic or hypoxic conditions for 72 hours and incubated with DAPI, MitoPy1 or MitoSox, and MitoTracker Red or MitoTracker Green. HPAECs were treated with 1000 U/mL PEG-Catalase or MitoTEMPO (100 nM) to confirm H_2O_2 or $O_2^{\bullet -}$ signal specificity, respectively. Chronic hypoxia increases MitoPY1 and MitoSox signals that were decreased by PEG-Catalase (Fig. 1A and 1B) and MitoTEMPO (Fig. 1C and 1D), respectively. These results indicate that hypoxia increases mitochondria-derived H_2O_2 and $O_2^{\bullet -}$.

Hypoxia increases Nox levels and proliferation markers in HPAECs

To determine if hypoxia modulates Nox we assessed hypoxia-induced mRNA and protein levels of Nox2 and Nox4. Hypoxia increased mRNA and protein levels of Nox2 (Fig. 2A and **representative blot**) and Nox4 (Fig. 2B and **representative blot**). Because increases in Nox2 and Nox4 have been shown to stimulate HPAEC growth and proliferation, we measured levels of cyclinD1 and PCNA [25, 38]. Hypoxia increased mRNA and protein levels of cyclinD1 (Fig. 2C and **representative blot**) and PCNA (Fig. 2D and **representative blot**), consistent with our previous findings that hypoxia elevates HPAEC proliferation [42].

Hypoxia-induced PH is attenuated in the MCAT model

To assess the role of mtH_2O_2 in hypoxia-induced PH, littermate control (Lit Cont) and MCAT mice [41] were studied. Human catalase expression was confirmed in MCAT mice (Fig. S1A – S1D). Hypoxia exposure significantly increased RVSP in littermate controls, however, the increase in RVSP was attenuated in MCAT mice (Fig. 3A). Hypoxia-induced changes in RVSP occurred independent of changes in heart rate (data not shown). In addition, compared to hypoxia-exposed Lit Cont, MCAT mice also demonstrated significantly less vascular remodeling, detected as α-SMA staining (Fig. 3B, 3C). Since vessel muscularization increases as vessel diameter increases, we ensured that all vessels measured were less than 100 μm in diameter, and that vessels of similar size from each group were compared (Fig. S2A). In contrast to the protective effects on RVSP and vessel muscularization, MCAT expression failed to attenuate hypoxia-induced RVH measured by either the Fulton Index, (Fig.3D) or echocardiography of right ventricular area (Fig. 3E). MCAT expression significantly attenuated hypoxia-induced elevations in H_2O_2 production (Fig. 3F). These results suggest that attenuating hypoxia-induced mtH_2O_2 generation reduces hypoxia-induced increases in RVSP and muscularization of small pulmonary vessels, without attenuating RVH.

Hypoxia-induced PH is exacerbated in the Tg^{hSOD2} model

To elucidate the effects of mt$O_2^{\bullet-}$ in the development of PH, we assessed the effect of SOD2 overexpression on PH. Human SOD2 expression was confirmed in the Tg^{hSOD2} model (Fig. S1E and S1F). Littermate control and Tg^{hSOD2} mice [43] were exposed to either normoxia or hypoxia. Tg^{hSOD2} mice had significantly higher RVSP when compared to normoxia exposed groups and hypoxia-exposed littermate controls (Fig 4A). No changes were detected in heart rate during RVSP measurement. Furthermore, compared to littermate controls, comparably sized vessels (Fig. S2B) in Tg^{hSOD2} mice had more α-SMA staining and thickening of the vascular wall (Fig. 4B and 4C). Tg^{hSOD2} expression had no significant effect on hypoxia-induced RVH (Fig. 4D) but exacerbated hypoxia-induced H_2O_2 production (Fig. 4E).

SOD2 and MCAT differentially affect hypoxia-induced Nox expression

Nox2 and Nox4 have been shown to contribute to physiological derangements seen in hypoxia-induced PH [44]. To determine if H_2O_2 levels impact Nox expression, we assessed Nox2 and Nox4 levels in lungs from MCAT and Tg^{hSOD2} mice. Nox2 mRNA and protein levels were attenuated in hypoxia-exposed MCAT pulmonary tissue (Fig. 5A and 5B). MCAT expression also prevented hypoxia-induced elevations in Nox4 mRNA and protein (Fig 5C and 5D). In contrast, SOD2 overexpression in the Tg^{hSOD2} model failed to prevent hypoxia-induced Nox2 mRNA and protein levels (Fig. 5E and 5F) and exacerbated hypoxia-induced Nox4 mRNA and protein levels (Fig. 5G and 5H). Furthermore, since Nox2 and Nox4 produce $O_2^{\bullet-}$ and H_2O_2, respectively, their elevation may account for the exacerbated H_2O_2 levels detected in the Tg^{hSOD2} model (Fig. 4E).

MCAT expression attenuates hypoxia-induced cyclinD1 and PCNA

The expression of cell cycle regulating proteins and proliferation markers were also evaluated. CyclinD1 regulates cell cycle progression and hypertrophy and promotes vascular cell proliferation and activation of PCNA [38, 45, 46]. MCAT expression prevented hypoxia-induced elevation of CyclinD1 when compared to normoxia controls (Fig. 6A). Furthermore, MCAT mice displayed less downstream hypoxia-induced proliferation as measured by PCNA protein expression in pulmonary tissue (Fig. 6B). In contrast, Tg^{hSOD2} mice displayed exacerbated cyclinD1 (Fig. 6C) and PCNA protein expression (Fig. 6D). Proliferation was also detected by PCNA IHC (Fig. S3).

DISCUSSION

The current studies demonstrate a vital contribution of mtH_2O_2 to the development of hypoxia-induced PH. As summarized in Fig. 7, hypoxia increases $mtO_2^{\bullet-}$ and mtH_2O_2 stimulating the expression and activity of Nox 2 and 4 and the physiological and molecular derangements seen in PH pathogenesis. These derangements in $mtO_2^{\bullet-}$ and mtH_2O_2 were targeted using Tg^{hSOD2} and MCAT models, respectively. Tg^{hSOD2} exacerbated hypoxia-induced H_2O_2 production and Nox 2 and 4 expression, and stimulated proliferation, muscularization, and increased RVSP. These same PH markers were attenuated in the MCAT model. Collectively, these studies demonstrate that targeted attenuation of mtH_2O_2 attenuates hypoxia-induced PH.

Hypoxia exposure increases RVSP [27, 28, 44], and the current study demonstrates that these hypoxia-induced elevations in RVSP are attenuated in the MCAT model and exacerbated in the SOD2 model. However, neither MCAT nor SOD2 attenuated hypoxia-induced elevations in RVH. Numerous studies suggest that exposure to chronic hypoxia elevates RVSP which subsequently leads to elevated RVH [47, 48]. In contrast, we have previously observed that attenuation of hypoxia-induced RVSP reduces RVH [27] or has no effect on RVH [28]. Our data indicate that the RVSP attenuation seen in hypoxic MCAT mice remained within the pulmonary hypertensive range. Therefore, while the decrease in RVSP was statistically significant, the pressures may have been sufficient to promote RVH. The physiological discrepancies between RVSP and RVH could also be due to differential expression of mitochondrial catalase in pulmonary and cardiac tissue. MCAT expression in cardiac tissue may not prevent hypoxia-induced RVH or targeting mtROS may promote RVH. For example, others have shown that super-suppression of H_2O_2 does not prevent cardiac hypertrophy [10]. Furthermore, smooth muscle cell-targeted knockout of HIF-1α, a transcription factor that contributes to pulmonary vascular remodeling and PH, prevented SMC remodeling and elevated pressures but not RVH [49, 50]. Collectively, these studies imply that cardiac hypertrophy may not be solely dependent on increases in pulmonary arterial pressure. Further studies assessing the molecular signaling of H_2O_2 in cardiac tissue are warranted to elucidate the potential mechanisms of RVH in PH.

The role of ROS in hypoxic pulmonary vasoconstriction has been controversial [13, 33, 35, 51], though growing support demonstrates that hypoxia stimulates mtROS generation [7, 52] which contributes to vascular dysfunction [31, 32]. Similar to previous studies [21, 38, 53], our confocal microscopy studies confirmed that hypoxia increases mtH_2O_2 and $mtO_2^{\bullet-}$ (Fig.

1A – 1D). Our studies also confirmed that MCAT expression reduced H_2O_2 release from pulmonary tissue (Fig. 2F), whereasH_2O_2 production was elevated in the hypoxic Tg^{hSOD2} model (Fig. 3E) [10]. Our study is consistent with data in a number of experimental models of PH that demonstrate an increase in $O_2^{\bullet-}$ levels [5, 27, 54] and oxidative stress biomarkers. Moreover, a growing body of work implicates mitochondria as sensors that detect changes in cellular O_2 levels. Mitochondria adjust intracellular redox-signaling pathways to modulate vascular tone and regulate hypoxia-induced redox signaling [8, 33–35].. Studies in fawn-hooded rat PASMC found a beneficial effect of elevated SOD2 [37], though overexpression of SOD2 to target $mtO_2^{\bullet-}$ led to an exacerbated PH phenotype in our study. Studies have confirmed that overexpression of SOD2 results in an increase in H_2O_2, as detected by the H_2O_2-sensitive dye, dichlorodihydrofluorescein diacetate (DCFDA) [55, 56]. It is our belief that overexpression of SOD2 increases the rate of dismutation of $mtO_2^{\bullet-}$ to mtH_2O_2, leading to elevated levels of mtH_2O_2. Furthermore, we posit that the exacerbated PH phenotype in the hypoxia Tg^{hSOD2} model is due to the increase in hypoxia-induced H_2O_2. It may be necessary that for SOD2 overexpression to be fully beneficial, an H_2O_2 scavenger may be needed in the same compartment [55–57]. These findings support our conclusions that mtH_2O_2 appears to drive PH vascular derangements.

$O_2^{\bullet-}$ and H_2O_2 play a vital role in vascular cell signaling [13] by regulating cellular proliferation, differentiation, and apoptosis [58] all of which lead to PH [59]. mtROS have been implicated in the pathophysiological and molecular proliferative and apoptotic derangements seen in vascular wall cells [7, 52, 60]. While other regulatory signaling pathways have been implicated in the derangements seen in PH, these pathways may be indirectly linked to the hypoxia-induced changes in H_2O_2 levels we observed. HIF-1α, NF-κB and other transcription factors have been shown to regulate vascular response to hypoxia and can be activated by H_2O_2 [39, 61, 62]. Similarly, H_2O_2 levels may drive vascular proliferation in PH [38] by regulating cyclinD1 and PCNA which promote cell proliferation[28, 38] and are increased with hypoxia exposure. These biochemical changes were attenuated in the MCAT model (Fig. 6A and 6B). These elevations are likely caused by hypoxia-induced increases in mtH_2O_2. This provides a link connecting mtROS, Noxes and the vascular proliferation seen in PH [5, 63].

Noxes, major sources of ROS within the vasculature [12, 13], regulate endothelial function, vascular tone, vascular cell hypertrophy, and apoptosis [14, 15]. Our study confirms previous observations that hypoxia induces Nox4 expression (Fig. 5C, 5D, 5G, and 5H) [17, 38, 44], and also demonstrates that hypoxia increases Nox2 (Fig. 5A, 5B, 5E, and 5F). While the regulation of mtROS and its effects on PH remain incompletely defined, some studies highlight that mtROS may stimulate Nox expression [36, 64]. Our study is the first to demonstrate that mtH_2O_2 directly contributes to induction of Nox2 and Nox4 expression. ROS generated by Noxes likely further contribute to aberrant pulmonary arterial responses. This process is supported by data which suggest that, in intrapulmonary arteries, hypoxia-induced endothelial dysfunction may be regulated by gp91phox/Nox2 and Nox4 [4, 54, 65, 66]. Accumulating evidence indicates that ROS derived from Nox2 and Nox4 are involved in long-term responses of the pulmonary vasculature to hypoxia [16, 65]. In studies using hypoxia models of PH, Nox2 KO mice demonstrated attenuated pulmonary artery superoxide generation and RVSP elevations. These data are consistent with data

demonstrating that hypoxia promotes mtROS which increases Nox2 levels [21, 67]. While these studies suggest that Nox2 expression is modulated by mtROS, other studies suggest that PH dysfunction may occur in a Nox2 independent manner [54]. In Nox4 KO mice, cardiac hypertrophy is attenuated and mitochondrial function is increased, solidifying the link between Nox4 and mtROS [68]. Our own studies using a Nox1/4 inhibitor support an important role for Nox4 in hypoxia-induced PH [28]. Though Nox4 mRNA upregulation in PH has been well demonstrated [25, 38, 39, 66], there remains debate regarding Nox4 localization to mitochondria [25, 69]. We are aware that ROS sources other than Noxes contribute to the acute or chronic responses to hypoxia and that we did not directly test the importance of these Noxes for chronic responses to hypoxia. We are also aware that Nox2 can modulate mtROS via complex I and that this mtROS contributes to elevated blood pressure [67]. Weissmann et al. revealed that sustained hypoxic pulmonary vasoconstriction (HPV) is dependent on mitochondrial complex I and IV and that Nox $p47^{phox}$-deficient mice were able to attenuate acute HPV [70]. Furthermore, previous studies have established that hypoxia-induced Nox4 plays an important role in the vascular remodeling, proliferation [17], and RVH [28] associated with PH development. Previous studies by our groups have shown that that inhibiting Nox1/4 attenuates PH and that PPARγ activation reduces Nox4 expression and PASMC proliferation [28, 39, 71]. Additionally, Noxes have been implicated in upregulation of cyclinD1 [72], possibly explaining the increased vascular proliferation seen in hypoxia-induced PH. We detected mtROS-mediated modulation of Noxes and cyclinD1, and PCNA but these studies are limited because we did not directly inhibit or knockdown Nox2 and Nox4 to demonstrate that PH and proliferation were attenuated. Nevertheless, our data are consistent with the concept that hypoxia-induced activation of mtH_2O_2 and Noxes contribute to elevation of cyclinD1 and PCNA, enhancing pulmonary vascular smooth muscle cell proliferation, vascular remodeling, and PH. Taken together these studies indicate the mtROS drives Nox expression which may in turn promote a proliferative pulmonary vascular cell phenotype [15, 25].

The Tg^{hSOD2} and MCAT models have several limitations. The models are limited by potential species-dependent responses to hypoxia. For example, hypoxia-induced PH rodent models fail to induce the proliferative, plexiform arteriopathy seen in patients with severe IPAH because the rodent models may not activate all of the signaling pathways that are active in PH pathobiology [73]. This hypoxia-induced rodent model of PH is appropriate for investigating Group 3 PH (associated with lung disease) [74]. Further, transgene expression in our models is not limited to vascular cells. Alveolar type I and type II epithelial cells and alveolar macrophages also express the transgene, and their dysregulation may contribute to hypoxia-induced PH. The Tg^{hSOD2} and MCAT models have been confirmed to improve mitochondrial function [40, 41], but this study aims to further our understanding of the role of mtROS in PH development. Despite limitations of murine models, hypoxia-induced PH in mice will continue to provide new insights into the pathobiology and treatment of PH [73, 75].

In summary, our results confirm that hypoxia increases $mtO_2^{\bullet -}$ and mtH_2O_2 and that mtH_2O_2 promotes hypoxia-induced PH by increasing Nox2, Nox4, cyclinD1, and PCNA. Inhibition of mtH_2O_2, with MCAT, prevented hypoxic induction of these molecular aberrations and many of the physiological derangements associated with PH, including

increased RVSP and vessel muscularization. Elevation of lung H_2O_2 in the hypoxic Tg^{hSOD2} model likely accounts for the exacerbation of the PH phenotype, proliferative markers, and muscularization (α-SMA). These studies encourage future PH treatments that target mitochondrial redox balance. Further examination of how mitochondria antioxidant overload modulates mitochondria function, which may exert major effects on vascular cell function, remain to be determined. To our knowledge, our study is the first to demonstrate that targeting mtH_2O_2 prevents both physiological and molecular derangments associated with hypoxia-induced PH. These results provide novel evidence for the involvement of mtH_2O_2 in the selective induction of Nox2 and Nox4 isoforms and maintenance of a proliferative pulmonary vascular cell phenotype.

Supplementary Material

Refer to Web version on PubMed Central for supplementary material.

ACKNOWLEDGEMENTS

We would like to express our thanks to Drs. Clintoria Richards-Williams, Jennifer Gooch, and Samantha Yeligar for their assistance during the preparation of the manuscript. The contents reported herein do not represent the views of the Department of Veterans Affairs or the United States Government.

SOURCES OF FUNDING

This work was supported by: NRSA 1F31HL114386 - 01A1 (SEA), NIH grant HL102167 (CMH/RLS), Graduate Training in the Pharmacological Sciences 5T32GM008602 (SEA), NIEHS Graduate and Postdoctoral Training in Toxicology PHS Grant 5T32ES12870-7 (SEA), and VA Merit Review 1I01BX001910 (CMH).

REFERENCES

1. Rabinovitch M. Molecular pathogenesis of pulmonary arterial hypertension. The Journal of clinical investigation. 2008; 118:2372–2379. [PubMed: 18596905]
2. Sakao S, Tatsumi K, Voelkel NF. Endothelial cells and pulmonary arterial hypertension: apoptosis, proliferation, interaction and transdifferentiation. Respir Res. 2009; 10:95. [PubMed: 19825167]
3. Weir EK, Archer SL. The role of redox changes in oxygen sensing. Respiratory physiology & neurobiology. 2010; 174:182–191. [PubMed: 20801237]
4. Fike CD, Slaughter JC, Kaplowitz MR, Zhang Y, Aschner JL. Reactive oxygen species from NADPH oxidase contribute to altered pulmonary vascular responses in piglets with chronic hypoxia-induced pulmonary hypertension. American journal of physiology. Lung cellular and molecular physiology. 2008; 295:L881–L888. [PubMed: 18757525]
5. Liu JQ, Folz RJ. Extracellular superoxide enhances 5-HT-induced murine pulmonary artery vasoconstriction. American Journal of Physiology - Lung Cellular and Molecular Physiology. 2004; 287:L111–L118. [PubMed: 15020294]
6. Mittal M, Gu XQ, Pak O, Pamenter ME, Haag D, Fuchs DB, Schermuly RT, Ghofrani HA, Brandes RP, Seeger W, Grimminger F, Haddad GG, Weissmann N. Hypoxia induces Kv channel current inhibition by increased NADPH oxidase-derived reactive oxygen species. Free Radical Biology and Medicine. 2007; 52:1033–1042. [PubMed: 22222468]
7. Chandel NS, Maltepe E, Goldwasser E, Mathieu CE, Simon MC, Schumacker PT. Mitochondrial reactive oxygen species trigger hypoxia-induced transcription. Proceedings of the National Academy of Sciences of the United States of America. 1998; 95:11715–11720. [PubMed: 9751731]
8. Guzy RD, Hoyos B, Robin E, Chen H, Liu L, Mansfield KD, Simon MC, Hammerling U, Schumacker PT. Mitochondrial complex III is required for hypoxia-induced ROS production and cellular oxygen sensing. Cell metabolism. 2005; 1:401–408. [PubMed: 16054089]

9. Waypa GB, Marks JD, Guzy R, Mungai PT, Schriewer J, Dokic D, Schumacker PT. Hypoxia triggers subcellular compartmental redox signaling in vascular smooth muscle cells. Circulation research. 2010; 106:526–535. [PubMed: 20019331]
10. Song M, Chen Y, Gong G, Murphy E, Rabinovitch PS, Dorn GW 2nd. Super-suppression of mitochondrial reactive oxygen species signaling impairs compensatory autophagy in primary mitophagic cardiomyopathy. Circulation research. 2014; 115:348–353. [PubMed: 24874428]
11. Wang YX, Zheng YM. ROS-dependent signaling mechanisms for hypoxic Ca(2+) responses in pulmonary artery myocytes. Antioxidants & redox signaling. 2010; 12:611–623. [PubMed: 19764882]
12. Sedeek M, Hebert RL, Kennedy CR, Burns KD, Touyz RM. Molecular mechanisms of hypertension: role of Nox family NADPH oxidases. Curr Opin Nephrol Hypertens. 2009; 18:122–127. [PubMed: 19430333]
13. Lyle AN, Griendling KK. Modulation of Vascular Smooth Muscle Signaling by Reactive Oxygen Species. Physiology. 2006; 21:269–280. [PubMed: 16868316]
14. Paravicini TM, Touyz RM. NADPH oxidases, reactive oxygen species, and hypertension: clinical implications and therapeutic possibilities. Diabetes Care. 2008; 31(Suppl 2):S170–S180. [PubMed: 18227481]
15. Dikalova AE, Bikineyeva AT, Budzyn K, Nazarewicz RR, McCann L, Lewis W, Harrison DG, Dikalov SI. Therapeutic targeting of mitochondrial superoxide in hypertension. Circulation research. 2010; 107:106–116. [PubMed: 20448215]
16. Frazziano G, Champion HC, Pagano PJ. NADPH oxidase-derived ROS and the regulation of pulmonary vessel tone. American journal of physiology. Heart and circulatory physiology. 2012; 302:H2166–H2177. [PubMed: 22427511]
17. Mittal M, Roth M, Konig P, Hofmann S, Dony E, Goyal P, Selbitz AC, Schermuly RT, Ghofrani HA, Kwapiszewska G, Kummer W, Klepetko W, Hoda MA, Fink L, Hanze J, Seeger W, Grimminger F, Schmidt HH, Weissmann N. Hypoxia-dependent regulation of nonphagocytic NADPH oxidase subunit NOX4 in the pulmonary vasculature. Circulation research. 2007; 101:258–267. [PubMed: 17585072]
18. Cutz E, Pan J, Yeger H. The role of NOX2 and "novel oxidases" in airway chemoreceptor O(2) sensing. Advances in experimental medicine and biology. 2009; 648:427–438. [PubMed: 19536508]
19. Bedard K, Krause KH. The NOX family of ROS-generating NADPH oxidases: physiology and pathophysiology. Physiological reviews. 2007; 87:245–313. [PubMed: 17237347]
20. Brown DI, Griendling KK. Nox proteins in signal transduction. Free radical biology & medicine. 2009; 47:1239–1253. [PubMed: 19628035]
21. Liu JQ, Erbynn EM, Folz RJ. Chronic hypoxia-enhanced murine pulmonary vasoconstriction: role of superoxide and gp91phox. Chest. 2005; 128:594S–596S. [PubMed: 16373854]
22. Liu JQ, Zelko IN, Erbynn EM, Sham JS, Folz RJ. Hypoxic pulmonary hypertension: role of superoxide and NADPH oxidase (gp91phox). American journal of physiology. Lung cellular and molecular physiology. 2006; 290:L2–L10. [PubMed: 16085672]
23. Ray R, Murdoch CE, Wang M, Santos CX, Zhang M, Alom-Ruiz S, Anilkumar N, Ouattara A, Cave AC, Walker SJ, Grieve DJ, Charles RL, Eaton P, Brewer AC, Shah AM. Endothelial Nox4 NADPH Oxidase Enhances Vasodilatation and Reduces Blood Pressure In Vivo. Arteriosclerosis, thrombosis, and vascular biology. 2011; 31:1368–1376.
24. Dikalov SI, Dikalova AE, Bikineyeva AT, Schmidt HH, Harrison DG, Griendling KK. Distinct roles of Nox1 and Nox4 in basal and angiotensin II-stimulated superoxide and hydrogen peroxide production. Free radical biology & medicine. 2008; 45:1340–1351. [PubMed: 18760347]
25. Frazziano G, Al Ghouleh I, Baust J, Shiva S, Champion HC, Pagano PJ. Nox-derived ROS are acutely activated in pressure overload pulmonary hypertension: indications for a seminal role for mitochondrial Nox4. American journal of physiology. Heart and circulatory physiology. 2014; 306:H197–H205. [PubMed: 24213612]
26. Sutliff RL, Kang BY, Hart CM. PPARgamma as a potential therapeutic target in pulmonary hypertension. Ther Adv Respir Dis. 2010; 4:143–160. [PubMed: 20530063]

27. Nisbet RE, Bland JM, Kleinhenz DJ, Mitchell PO, Walp ER, Sutliff RL, Hart CM. Rosiglitazone Attenuates Chronic Hypoxia-Induced Pulmonary Hypertension in a Mouse Model. Am. J. Respir. Cell Mol. Biol. 2010; 42:482–490. [PubMed: 19520921]

28. Green DE, Murphy TC, Kang B-Y, Kleinhenz JM, Szyndralewiez C, Page P, Sutliff RL, Hart CM. The Nox4 Inhibitor GKT137831 Attenuates Hypoxia- Induced Pulmonary Vascular Cell Proliferation. American Journal of Respiratory Cell and Molecular Biology. 2012; 47:718–726. [PubMed: 22904198]

29. Dikalov S. Cross talk between mitochondria and NADPH oxidases. Free Radic Biol Med. 2011; 51:1289–1301. [PubMed: 21777669]

30. Aon MA, Cortassa S, O'Rourke B. Redox-optimized ROS balance: A unifying hypothesis. Biochimica et Biophysica Acta (BBA) - Bioenergetics. 2010; 1797:865–877. [PubMed: 20175987]

31. Min W, Xu LK, Zhou HJ, Huang Q, Zhang H, He Y, Zhe X, Y L. Thioredoxin and redox signaling in vasculature-studies using Trx2 endothelium-specific transgenic mice. Methods Enzymology. 2010; 474:315–324.

32. Widder JD, Fraccarollo D, Galuppo P, Hansen JM, Jones DP, Ertl G, Bauersachs J. Attenuation of angiotensin II-induced vascular dysfunction and hypertension by overexpression of Thioredoxin 2. Hypertension. 2009; 54:338–344. [PubMed: 19506101]

33. Fuchs B, Sommer N, Dietrich A, Schermuly RT, Ghofrani HA, Grimminger F, Seeger W, Gudermann T, Weissmann N. Redox signaling and reactive oxygen species in hypoxic pulmonary vasoconstriction. Respiratory physiology & neurobiology. 2010; 174:282–291. [PubMed: 20801235]

34. Waypa GB, Schumacker PT. Hypoxia-induced changes in pulmonary and systemic vascular resistance: Where is the O2 sensor? Respiratory physiology & neurobiology. 2010; 174:201–211. [PubMed: 20713189]

35. Shimoda LA, Undem C. Interactions between calcium and reactive oxygen species in pulmonary arterial smooth muscle responses to hypoxia. Respiratory Physiology & Neurobiology. 2010; 174:221–229. [PubMed: 20801238]

36. Dikalov S. Cross talk between mitochondria and NADPH oxidases. Free radical biology & medicine. 2011

37. Archer SL, Marsboom G, Kim GH, Zhang HJ, Toth PT, Svensson EC, Dyck JRB, Gomberg-Maitland M, Theobaud B, Husain AN, Cipriani N, Rehman J. Epigenetic attenuation of mitochondrial superoxide dismutase 2 in pulmonary arterial hypertension. Circulation. 2010; 121:2661–2671. [PubMed: 20529999]

38. Wedgwood S, Lakshminrusimha S, Czech L, Schumacker PT, Steinhorn RH. Increased p22(phox)/Nox4 expression is involved in remodeling through hydrogen peroxide signaling in experimental persistent pulmonary hypertension of the newborn. Antioxidants & redox signaling. 2013; 18:1765–1776. [PubMed: 23244636]

39. Lu X, Bijli KM, Ramirez A, Murphy TC, Kleinhenz J, Hart CM. Hypoxia downregulates PPARgamma via an ERK1/2-NF-kappaB-Nox4-dependent mechanism in human pulmonary artery smooth muscle cells. Free radical biology & medicine. 2013; 63:151–160. [PubMed: 23684777]

40. Jang YC, Perez VI, Song W, Lustgarten MS, Salmon AB, Mele J, Qi W, Liu Y, Liang H, Chaudhuri A, Ikeno Y, Epstein CJ, Van Remmen H, Richardson A. Overexpression of Mn superoxide dismutase does not increase life span in mice. The journals of gerontology. Series A, Biological sciences and medical sciences. 2009; 64:1114–1125.

41. Schriner SE, Linford NJ, Martin GM, Treuting P, Ogburn CE, Emond M, Coskun PE, Ladiges W, Wolf N, Van Remmen H, Wallace DC, Rabinovitch PS. Extension of murine life span by overexpression of catalase targeted to mitochondria. Science. 2005; 308:1909–1911. [PubMed: 15879174]

42. Porter KM, Kang BY, Adesina SE, Murphy TC, Hart CM, Sutliff RL. Chronic hypoxia promotes pulmonary artery endothelial cell proliferation through H2O2-induced 5-lipoxygenase. PloS one. 2014; 9:e98532. [PubMed: 24906007]

43. Kowluru RA, Kowluru V, Xiong Y, Ho Y-S. Overexpression of mitochondrial superoxide dismutase in mice protects the retina from diabetes-induced oxidative stress. Free Radical Biology and Medicine. 2006; 41:1191–1196. [PubMed: 17015165]

44. Nisbet RE, Graves AS, Kleinhenz DJ, Rupnow HL, Reed AL, Fan TH, Mitchell PO, Sutliff RL, Hart CM. The role of NADPH oxidase in chronic intermittent hypoxia-induced pulmonary hypertension in mice. Am J Respir Cell Mol Biol. 2009; 40:601–609. [PubMed: 18952568]
45. Samaga KK, Rao GV, Chandrashekara Reddy G, Kush AK, Diwakar L. Synthetic racemates of abyssinone I and II induces apoptosis through mitochondrial pathway in human cervix carcinoma cells. Bioorganic chemistry. 2014; 56C:54–61. [PubMed: 25019692]
46. Jing L, Peng X, Xie MJ, Yu ZY, Wang W. Different responses of cell cycle between rat vascular smooth muscle cells and vascular endothelial cells to paclitaxel. Journal of Huazhong University of Science and Technology. Medical sciences = Hua zhong ke ji da xue xue bao. Yi xue Ying De wen ban = Huazhong keji daxue xuebao. Yixue Yingdewen ban. 2014; 34:370–375.
47. Hoshikawa Y, Ono S, Suzuki S, Tanita T, Chida M, Song C, Noda M, Tabata T, Voelkel NF, Fujimura S. Generation of oxidative stress contributes to the development of pulmonary hypertension induced by hypoxia. Journal of applied physiology. 2001; 90:1299–1306. [PubMed: 11247927]
48. Porter KM, Walp ER, Elms SC, Raynor R, Mitchell PO, Guidot DM, Sutliff RL. Human immunodeficiency virus-1 transgene expression increases pulmonary vascular resistance and exacerbates hypoxia-induced pulmonary hypertension development. Pulmonary circulation. 2013; 3:58–67. [PubMed: 23662175]
49. Smith KA, Yuan JXJ. Hypoxia-Inducible Factor-1α in Pulmonary Arterial Smooth Muscle Cells and Hypoxia-induced Pulmonary Hypertension. American journal of respiratory and critical care medicine. 2014; 189:245–246. [PubMed: 24484328]
50. Ball MK, Waypa GB, Mungai PT, Nielsen JM, Czech L, Dudley VJ, Beussink L, Dettman RW, Berkelhamer SK, Steinhorn RH, Shah SJ, Schumacker PT. Regulation of hypoxia-induced pulmonary hypertension by vascular smooth muscle hypoxia-inducible factor-1alpha. American journal of respiratory and critical care medicine. 2014; 189:314–324. [PubMed: 24251580]
51. Wolin, MS.; Ahmad, M.; Gupte, SA. Role of Oxygen-Derived Species in the Regulation of Pulmonary Vascular Tone. In: Yuan, JX-J., et al., editors. Textbook of Pulmonary Vascular Disease. New York: Springer; 2011. p. 301-311.
52. Waypa GB, Marks JD, Guzy RD, Mungai PT, Schriewer JM, Dokic D, Ball MK, Schumacker PT. Superoxide generated at mitochondrial complex III triggers acute responses to hypoxia in the pulmonary circulation. American journal of respiratory and critical care medicine. 2013; 187:424–432. [PubMed: 23328522]
53. Wedgwood S, Lakshminrusimha S, Fukai T, Russell JA, Schumacker PT, RH S. Hydrogen peroxide regulates extracellular superoxide dismutase activity and expression in neonatal pulmonary hypertension. Antioxidant Redox Signal. 2011; 15:1497–1506.
54. Fresquet F, Pourageaud F, Leblais V, Brandes RP, Savineau JP, Marthan R, Muller B. Role of reactive oxygen species and gp91phox in endothelial dysfunction of pulmonary arteries induced by chronic hypoxia. British journal of pharmacology. 2006; 148:714–723. [PubMed: 16715116]
55. Connor KM, Subbaram S, Regan KJ, Nelson KK, Mazurkiewicz JE, Bartholomew PJ, Aplin AE, Tai YT, Aguirre-Ghiso J, Flores SC, Melendez JA. Mitochondrial H2O2 regulates the angiogenic phenotype via PTEN oxidation. The Journal of biological chemistry. 2005; 280:16916–16924. [PubMed: 15701646]
56. Dasgupta J, Subbaram S, Connor KM, Rodriguez AM, Tirosh O, Beckman JS, Jourd'Heuil D, Melendez JA. Manganese superoxide dismutase protects from TNF-alpha-induced apoptosis by increasing the steady-state production of H2O2. Antioxidants & redox signaling. 2006; 8:1295–1305. [PubMed: 16910777]
57. Usui S, Oveson BC, Iwase T, Lu L, Lee SY, Jo YJ, Wu Z, Choi EY, Samulski RJ, Campochiaro PA. Overexpression of SOD in retina: need for increase in H2O2-detoxifying enzyme in same cellular compartment. Free radical biology & medicine. 2011; 51:1347–1354. [PubMed: 21736939]
58. Watson WH, Chen Y, Jones DP. Redox state of glutathione and thioredoxin in differentiation and apoptosis. BioFactors. 2003; 17:307–314. [PubMed: 12897452]
59. Blanquicett C, Kang B-Y, Ritzenthaler JD, Jones DP, Hart CM. Oxidative stress modulates PPARgamma] in vascular endothelial cells. Free Radical Biology and Medicine. 2010; 48:1618–1625. [PubMed: 20302927]

60. Gillespie MN, Al-Mehdi AB, McMurtry IF. Mitochondria in hypoxic pulmonary vasoconstriction: potential importance of compartmentalized reactive oxygen species signaling. American journal of respiratory and critical care medicine. 2013; 187:338–340. [PubMed: 23418325]

61. Shimoda LA, Semenza GL. HIF and the lung: role of hypoxia-inducible factors in pulmonary development and disease. American journal of respiratory and critical care medicine. 2011; 183:152–156. [PubMed: 21242594]

62. Brusselmans K, Compernolle V, Tjwa M, Wiesener MS, Maxwell PH, Collen D, Carmeliet P. Heterozygous deficiency of hypoxia-inducible factor-2alpha protects mice against pulmonary hypertension and right ventricular dysfunction during prolonged hypoxia. The Journal of clinical investigation. 2003; 111:1519–1527. [PubMed: 12750401]

63. Wedgwood S, Black SM. Molecular mechanisms of nitric oxide-induced growth arrest and apoptosis in fetal pulmonary arterial smooth muscle cells. Nitric Oxide. 2003; 9:201–210. [PubMed: 14996427]

64. Dikalov SI, Ungvari Z. Role of mitochondrial oxidative stress in hypertension. American journal of physiology. Heart and circulatory physiology. 2013; 305:H1417–H1427. [PubMed: 24043248]

65. Griffith B, Pendyala S, Hecker L, Lee PJ, Natarajan V, Thannickal VJ. NOX enzymes and pulmonary disease. Antioxidants & redox signaling. 2009; 11:2505–2516. [PubMed: 19331546]

66. Barman SA, Chen F, Su Y, Dimitropoulou C, Wang Y, Catravas JD, Han W, Orfi L, Szantai-Kis C, Keri G, Szabadkai I, Barabutis N, Rafikova O, Rafikov R, Black SM, Jonigk D, Giannis A, Asmis R, Stepp DW, Ramesh G, Fulton DJ. NADPH oxidase 4 is expressed in pulmonary artery adventitia and contributes to hypertensive vascular remodeling. Arteriosclerosis, thrombosis, and vascular biology. 2014; 34:1704–1715.

67. Khan SA, Nanduri J, Yuan G, Kinsman B, Kumar GK, Joseph J, Kalyanaraman B, Prabhakar NR. NADPH oxidase 2 mediates intermittent hypoxia-induced mitochondrial complex I inhibition: relevance to blood pressure changes in rats. Antioxidants & redox signaling. 2011; 14:533–542. [PubMed: 20618070]

68. Kuroda J, Ago T, Matsushima S, Zhai P, Schneider MD, Sadoshima J. NADPH oxidase 4 (Nox4) is a major source of oxidative stress in the failing heart. Proceedings of the National Academy of Sciences of the United States of America. 2010; 107:15565–15570. [PubMed: 20713697]

69. Ago T, Kuroda J, Pain J, Fu C, Li H, Sadoshima J. Upregulation of Nox4 by hypertrophic stimuli promotes apoptosis and mitochondrial dysfunction in cardiac myocytes. Circulation research. 2010; 106:1253–1264. [PubMed: 20185797]

70. Weissmann N, Zeller S, Schafer RU, Turowski C, Ay M, Quanz K, Ghofrani HA, Schermuly RT, Fink L, Seeger W, Grimminger F. Impact of mitochondria and NADPH oxidases on acute and sustained hypoxic pulmonary vasoconstriction. Am J Respir Cell Mol Biol. 2006; 34:505–513. [PubMed: 16357364]

71. Bijli KM, Kleinhenz JM, Murphy TC, Kang BY, Adesina SE, Sutliff RL, Hart CM. Peroxisome proliferator-activated receptor gamma depletion stimulates Nox4 expression and human pulmonary artery smooth muscle cell proliferation. Free radical biology & medicine. 2015; 80:111–120. [PubMed: 25557278]

72. Veit F, Pak O, Egemnazarov B, Roth M, Kosanovic D, Seimetz M, Sommer N, Ghofrani HA, Seeger W, Grimminger F, Brandes RP, Schermuly RT, Weissmann N. Function of NADPH Oxidase 1 in Pulmonary Arterial Smooth Muscle Cells After Monocrotaline-Induced Pulmonary Vascular Remodeling. Antioxidants & redox signaling. 2013

73. Stenmark KR, Meyrick B, Galie N, Mooi WJ, McMurtry IF. Animal models of pulmonary arterial hypertension: the hope for etiological discovery and pharmacological cure. American Journal of Physiology - Lung Cellular and Molecular Physiology. 2009; 297:L1013–L1032. [PubMed: 19748998]

74. Ryan J, Bloch K, Archer SL. Rodent models of pulmonary hypertension: harmonisation with the world health organisation's categorisation of human PH. International journal of clinical practice. Supplement. 2011:15–34. [PubMed: 21736677]

75. Bauer NR, Moore TM, McMurtry IF. Rodent models of PAH: are we there yet?. 2007

HIGHLIGHTS

Our results confirm that hypoxia increases mitochondrial $O_2^{\bullet -}$ and H_2O_2 production.

Our findings further demonstrate that mitochondrial $O_2^{\bullet -}$ and mitochondrial H_2O_2 participate in hypoxia-induced expression and activity of Nox2 and Nox4 *in vivo*.

Targeted attenuation of mitochondrial H_2O_2 prevents hypoxia-induced elevation of RVSP, vessel muscularization, Nox2, Nox4, cyclinD1, and PCNA mRNA and protein, whereas targeted attenuation of mitochondrial $O_2^{\bullet -}$ exacerbated those markers.

These studies thereby provide novel evidence that targeting mitochondrial H_2O_2 prevents both physiological and molecular derangments associated with hypoxia-induced PH.

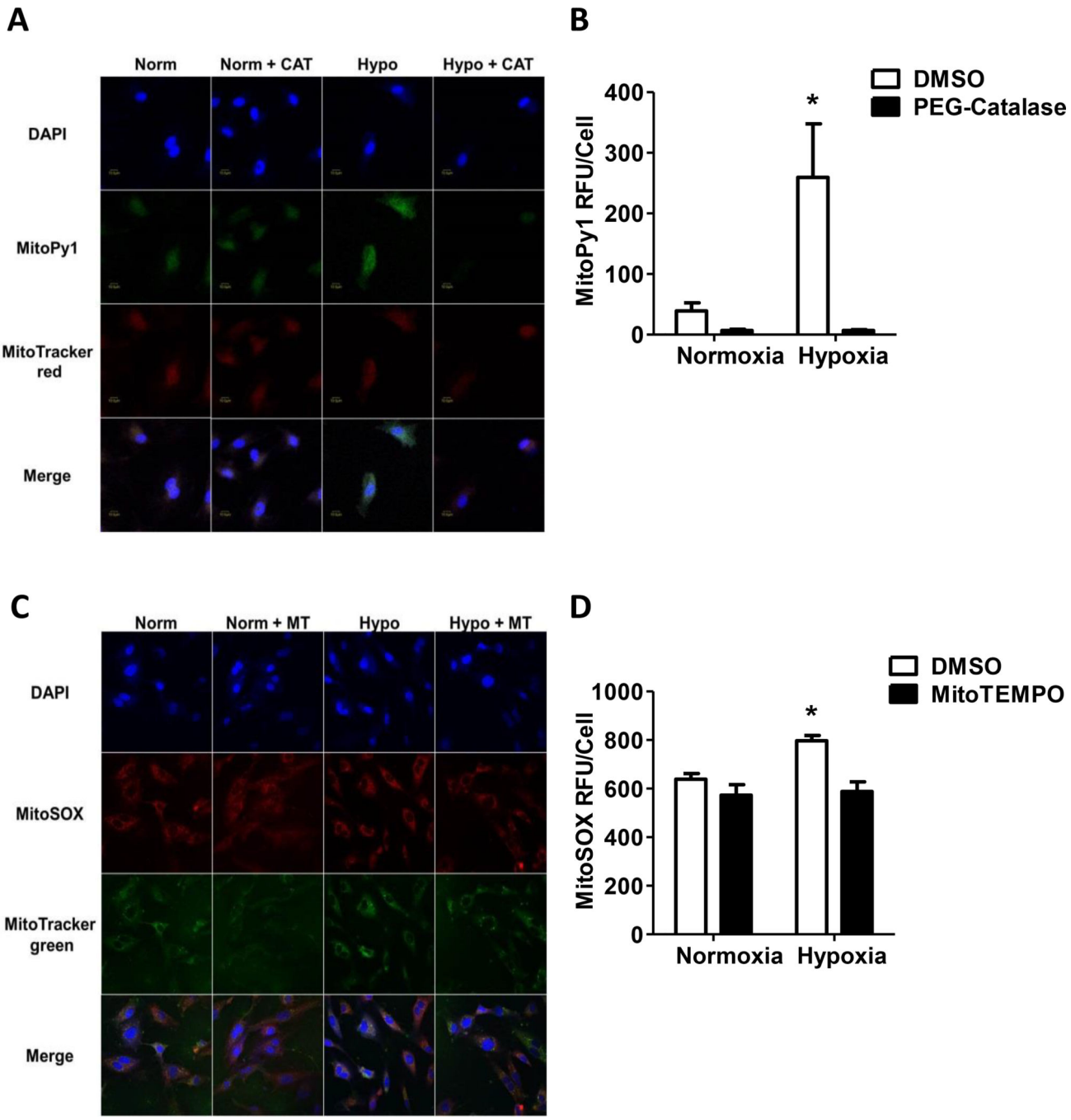

Figure 1. Hypoxia increases mtROS generation, Nox2, Nox4, CyclinD1, and PCNA mRNA in HPAECs

HPAECs were exposed to normoxia (21%O_2) or hypoxia (1%O_2) for 72 hours. Following exposure, cells were assessed for mitochondrial $O_2^{\bullet -}$ and H_2O_2 by confocal microscopy. **(A)** HPAECs were treated with 1000 U/mL PEG-catalase or DMSO vehicle during the last 24 hours of exposure, treated with MitoPy1, MitroTracker red, and Dapi. Representative images at 90× magnification presented, scale bar 10 μm. **(B)** The fluorescence intensity in 50 – 100 cells from each treatment group and is presented as mean ± SEM MitoPy1 relative

fluorescence units (RFU)/cell. PEG-Catalase treatment prevents hypoxia induced mtH_2O_2 production (n = 3), *p < 0.05 compared to all other groups. **(C)** HPAECs were treated with 100 nM MitoTEMPO or DMSO vehicle daily and then treated with MitoSOX, MitoTracker green, and DAPI. Representative images at 90× magnification. **(D)** The fluorescence intensity in each treatment group was measured in 50 – 100 cells and is presented as mean ± SEM MitoSOX RFU/cell. MitoTEMPO treatment prevents hypoxia induced mt$O_2^{\bullet -}$ production (n = 3), *p < 0.05 compared to all other groups.

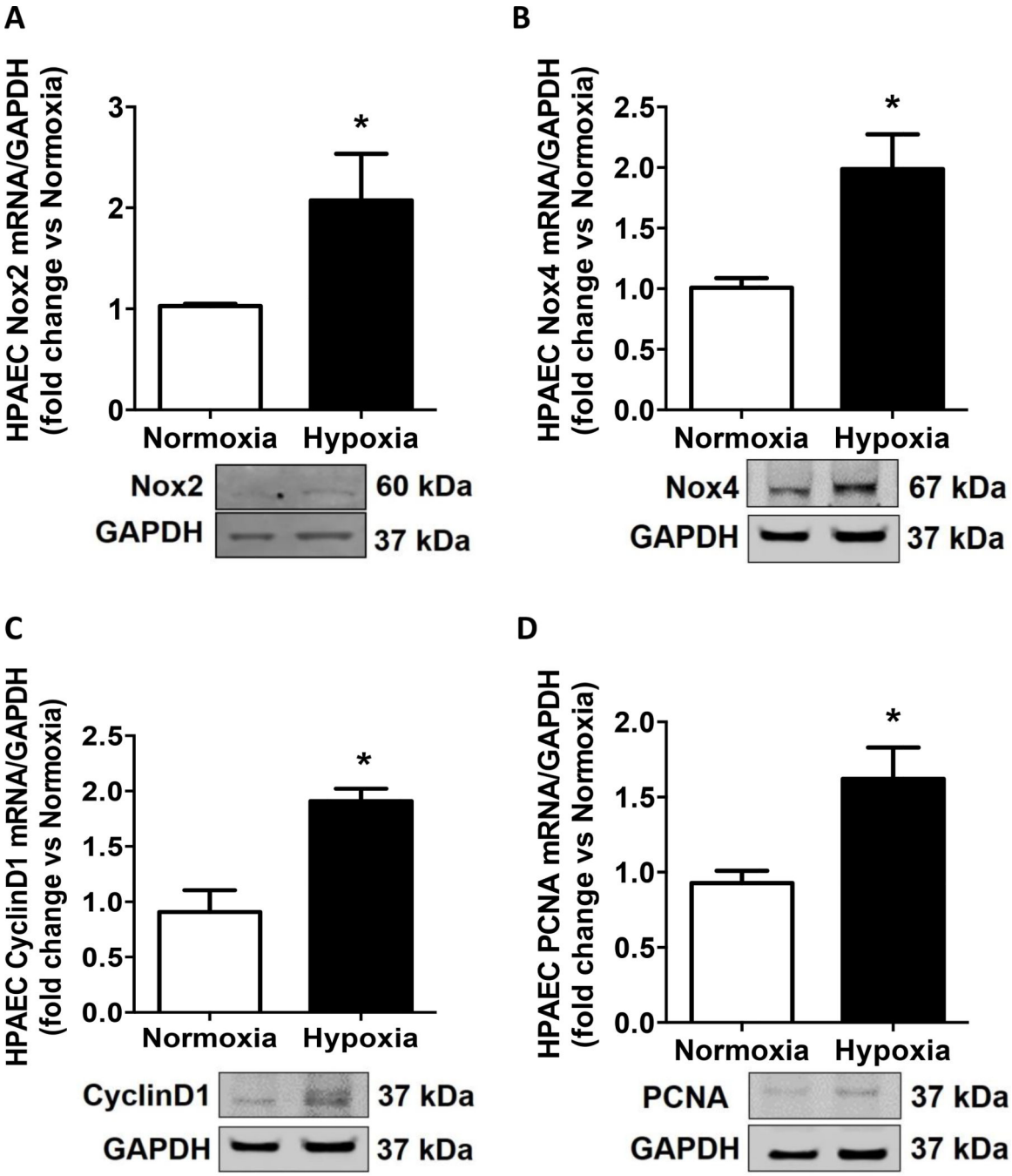

Figure 2. Hypoxia increases Nox2, Nox4, CyclinD1, and PCNA mRNA and protein in HPAECs

HPAECs were exposed to normoxia (21%O_2) or hypoxia (1%O_2) for 72 hours. Following exposure, cells were harvested and Nox expression and proliferation markers were assessed by qRT-PCR (relative to GAPDH expressed as fold-change vs. Normoxia) and western blot (normalized to GAPDH). Hypoxia increases expression levels of **(A)** Nox2 and **(B)** Nox4 and increases levels of the proliferation markers **(C)** cyclinD1 and **(D)** PCNA. Each bar represents mean ± SEM (n = 3), *p < 0.05 compared to Normoxia.

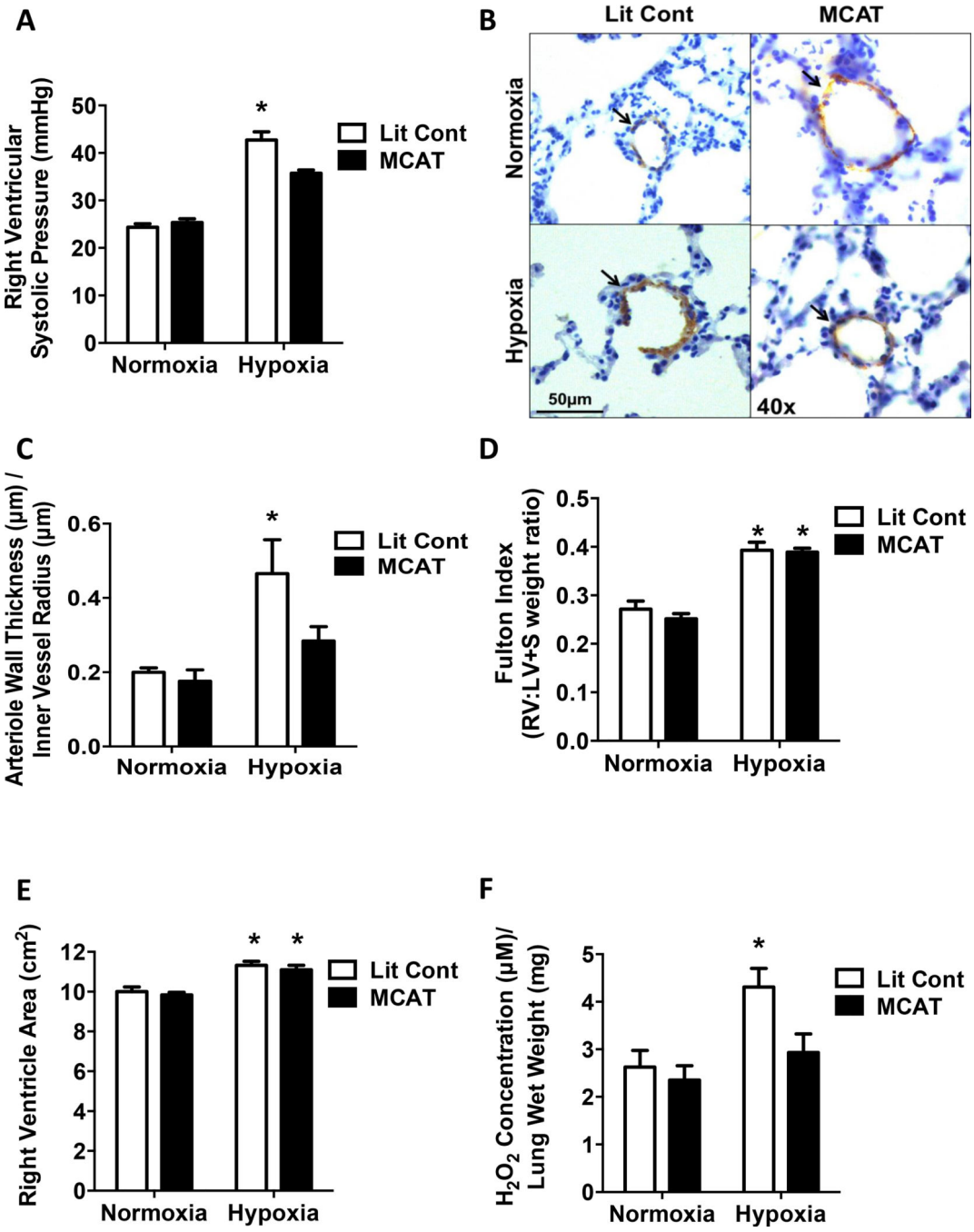

Figure 3. Mitochondrial-targeted catalase overexpression attenuates hypoxia-induced PH and muscularization of small pulmonary arteries

Littermate control (Lit Cont) and MCAT mice were exposed normoxia (21% O_2) or hypoxia (10% O_2) for 3-weeks in 3 separate studies. **(A)** Right ventricular systolic pressure (RVSP) was recorded with a pressure transducer. MCAT expression able to prevent hypoxia-induced elevations in RVSP. Each bar represents mean ± SEM RVSP in mmHg (n = 10), *$p < 0.05$ compared to all other groups. **(B)** Lung sections (5 μm thick) were stained with α-SMA. Representative images are displayed as indicated. Brown staining indicated by arrows

represents α-SMA positive staining in the media of small pulmonary arterioles. Magnification = 40×. **(C)** The wall thickness calculated by dividing total thickness of vessel by inner vessel radius. MCAT expression able to prevent hypoxia-induced elevations in α-SMA staining of small arterioles (n = 3 – 4), *p < 0.05 compared to all other groups. **(D)** Right ventricular hypertrophy was assessed by dissecting and weighing the right ventricle (RV) and the left ventricle + septum (LV + S) and calculating the RV:LV+S weight ratio. Hypoxia induces elevations in RVH. Each bar represents the mean ± SEM RV:LV+S weight ratio (n = 7 – 8), *p < 0.05 compared to both normoxia groups. **(E)** Right ventricular hypertrophy was also assessed by cardiac echocardiography and measurement of the right ventricular area. Each bar represents mean ± SEM RV area in cm^2. Hypoxia increases right ventricular area (n = 7 – 8), *p < 0.05 compared to both normoxia groups. Amplex Red assay was utilized to assess lung extracellular H_2O_2 levels in lung tissue. **(F)** MCAT expression significantly decreased hypoxia-induced H_2O_2 production. Each bar represents mean ± SEM H_2O_2 concentration relative to lung tissue wet weight (n = 5 – 6), *p < 0.05 compared to all other groups.

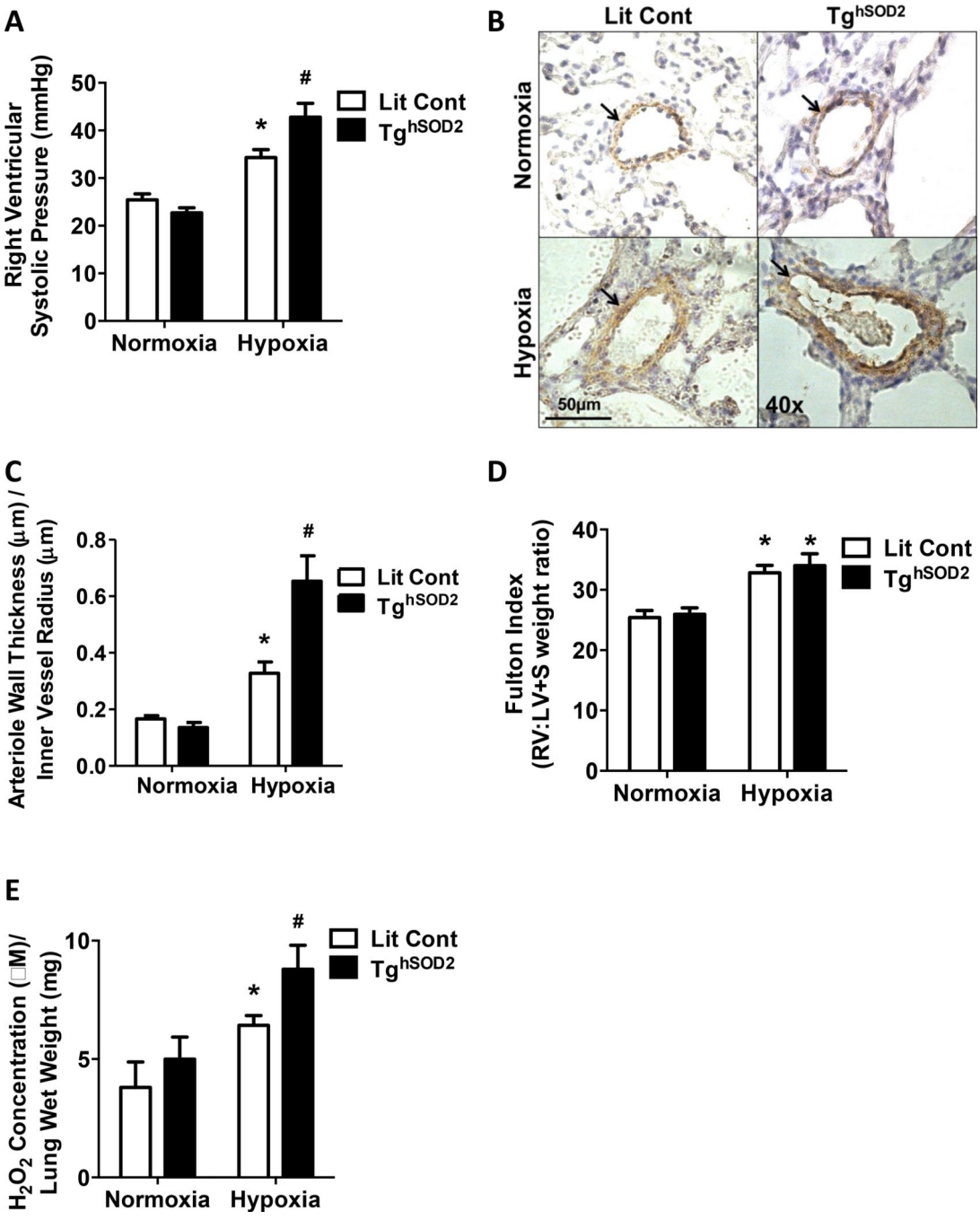

Figure 4. SOD2 overexpression exacerbates hypoxia-induced RVSP, RVH, and muscularization of small pulmonary arteries

Littermate control (Lit Cont) and Tg^{hSOD2} mice were exposed normoxia (21% O_2) or hypoxia (10% O_2) for 3-weeks in 2 independent studies. **(A)** RVSP was recorded with a pressure transducer. Hypoxia elevates RVSPs, which is exacerbated in Tg^{hSOD2} mice. Each bar represents mean ± SEM RVSP in mm Hg (n = 4 – 5), *$p < 0.05$ compared to Lit Cont Normoxia and $^{\#}p < 0.05$ compared to Lit Cont Hypoxia. **(B)** Lung sections (5 μm thick) were stained with α-SMA. Representative images are displayed as indicated. Brown staining

indicated by arrows represents α-SMA positive staining in the media of small pulmonary arterioles. Magnification = 40×. **(C)** The wall thickness calculated by dividing total thickness of vessel by inner vessel radius. Tg^{hSOD2} mice has exacerbated hypoxia-induced α-SMA staining of small arterioles (n = 3), *p < 0.05 compared to Lit Cont Normoxia and $^{\#}p < 0.05$ compared to Lit Cont Hypoxia. **(D)** Tg^{hSOD2} expression had no significant effect on hypoxia-induced RVH. Each bar represents the mean ± SEM RV:LV+S weight ratio (n = 8 – 12), *p < 0.05 compared to both Normoxia groups. **(E)** Tg^{hSOD2} expression significantly increased hypoxia- induced H_2O_2 production. Each bar represents mean ± SEM H_2O_2 concentration relative to lung tissue wet weight (n = 5 – 9), *p < 0.05 compared to Lit Cont Normoxia and $^{\#}p < 0.05$ compared to Lit Cont Hypoxia.

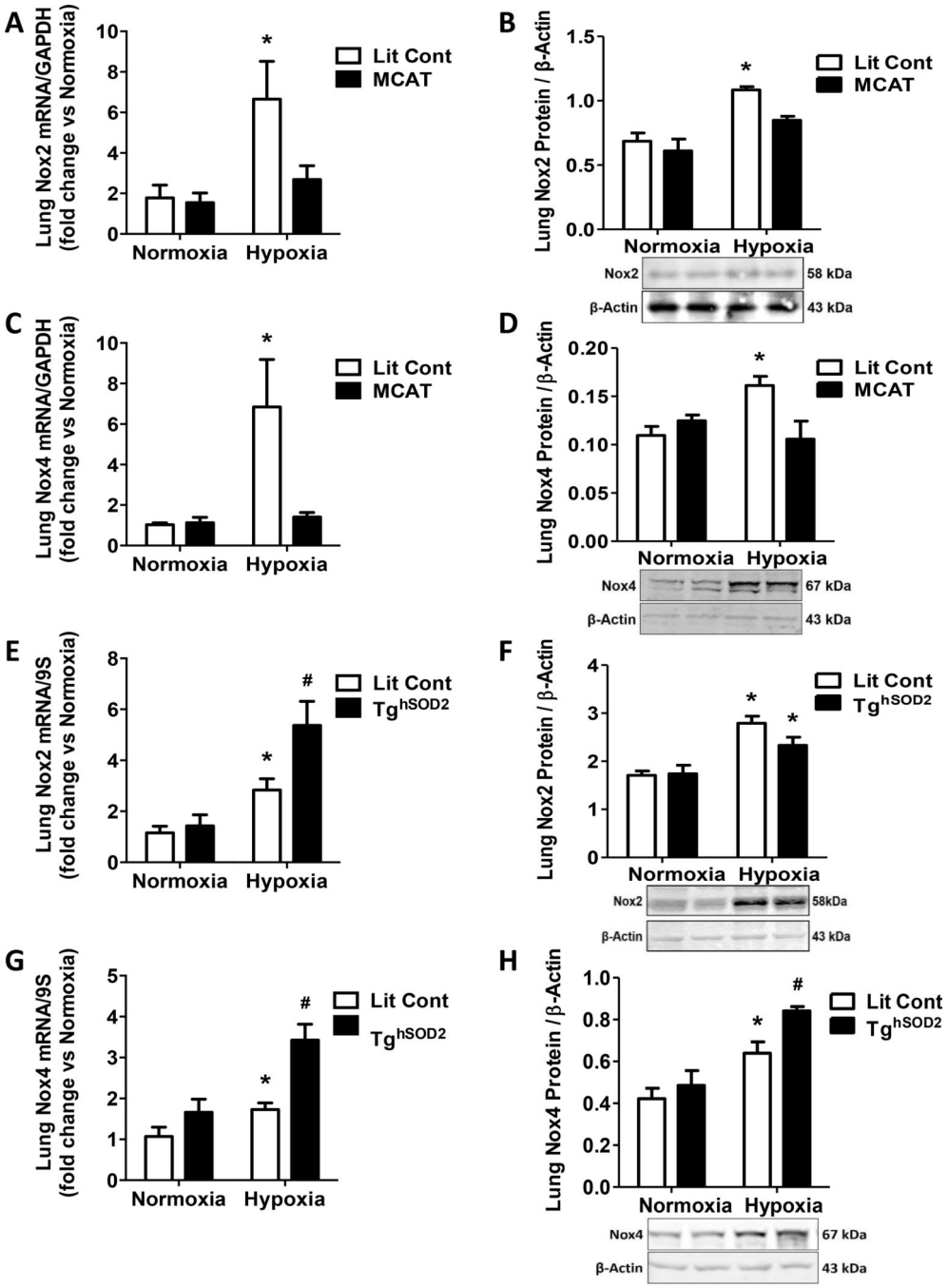

Figure 5. mtH_2O_2 attenuation prevents hypoxia-induced Nox expression

Lit Cont and MCAT mice were exposed to normoxic or hypoxic conditions for 3 weeks. Whole lung homogenates were collected from Lit Cont, MCAT, and Tg^{hSOD2} mice. Nox mRNA values are relative to GAPDH, or 9S and expressed as fold-change vs. Normoxia. Protein samples are normalized to β-Actin. **(A)** MCAT expression attenuated hypoxiainduced Nox2 mRNA. Each bar represents mean ± SEM lung Nox2 mRNA (n = 9), *p < 0.05 compared to all other groups. **(B)** MCAT expression inhibited hypoxia-induced Nox2 protein levels. Each bar represents mean ± SEM lung Nox2 protein (n = 2 – 3), *p <

0.05 compared to all other groups. **(C)** MCAT expression prevented elevation of hypoxia-induced Nox4 mRNA levels. Each bar represents mean ± SEM lung Nox4 mRNA (n = 7 – 10), *p < 0.05 compared to all other groups. **(D)** Nox4 hypoxia-induced protein expression was attenuated in MCAT mice. Each bar represents mean ± SEM lung Nox4 protein (n = 3 – 4), *p < 0.05 compared to all other groups. **(E)** Hypoxia-induced lung Nox2 mRNA expression was exacerbated in Tg^{hSOD2}. Each bar represents mean ± SEM lung Nox2 mRNA (n = 6 – 11), *p < 0.05 compared to Lit Cont Normoxia and $^{\#}p < 0.05$ compared to Lit Cont Hypoxia. **(F)** Hypoxia elevates lung Nox2 protein in both Lit Cont and Tg^{hSOD2}. Each bar represents mean ± SEM lung Nox2 protein (n = 3), *p < 0.05 compared to all other groups. **(G)** Hypoxia-induced Nox4 mRNA expression is exacerbated in hypoxia-exposed Tg^{hSOD2}. Each bar represents mean ± SEM lung Nox4 mRNA (n = 6), *p < 0.05 compared to Lit Cont Normoxia and $^{\#}p < 0.05$ compared to Lit Cont Hypoxia. **(H)** Hypoxia increases lung Nox4 protein in Lit Cont and this increase is exacerbated in the hypoxia Tg^{hSOD2} model. Each bar represents mean ± SEM lung Nox4 protein (n = 3 – 4), *p < 0.05 compared to Lit Cont Normoxia and $^{\#}p < 0.05$ compared to Lit Cont Hypoxia.

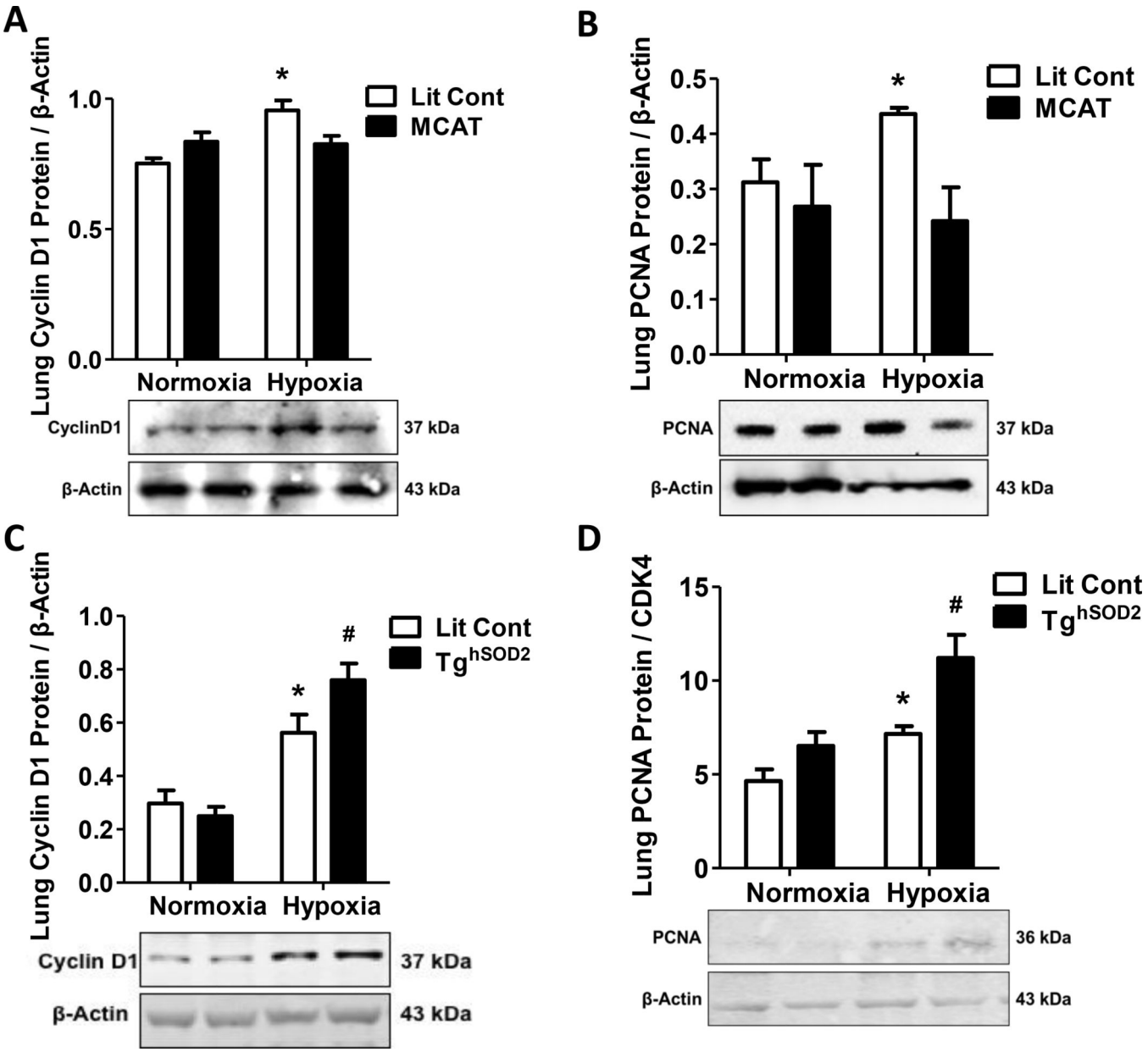

Figure 6. Targeted attenuation of mtH_2O_2 prevents hypoxia-induced proliferation

Lit Cont and transgenic mice were exposed to normoxic or hypoxic conditions for 3 weeks. Whole lung homogenates were collected from Lit Cont, MCAT, and Tg^{hSOD2} mice. MCAT expression prevented hypoxia-induced induction of cyclinD1 and PCNA protein expression. CyclinD1 and PCNA values are normalized to β-Actin or CDK4. **(A)** MCAT expression inhibited hypoxia-induced elevation of cyclinD1 protein. Each bar represents mean ± SEM lung cyclinD1 protein (n = 5 – 6), *p < 0.05 compared to all other groups. **(B)** MCAT expression inhibited hypoxia-induced elevation of PCNA protein. Each bar represents mean ± SEM lung PCNA protein (n =3 – 5), *p < 0.05 compared to all other groups. **(C)** Tg^{hSOD2} mice displayed exacerbated hypoxia-induced cyclinD1 protein expression. Each bar represents mean ± SEM lung cyclinD1 protein (n = 3 – 5), *p < 0.05 compared to Lit Cont

Normoxia and $^{\#}p < 0.05$ compared to Lit Cont Hypoxia. **(D)** Tg^{hSOD2} mice also displayed exacerbated hypoxia-induced PCNA protein expression. Each bar represents mean ± SEM lung PCNA protein (n =3 – 6), $^{*}p < 0.05$ compared to Lit Cont Normoxia and $^{\#}p < 0.05$ compared to Lit Cont Hypoxia.

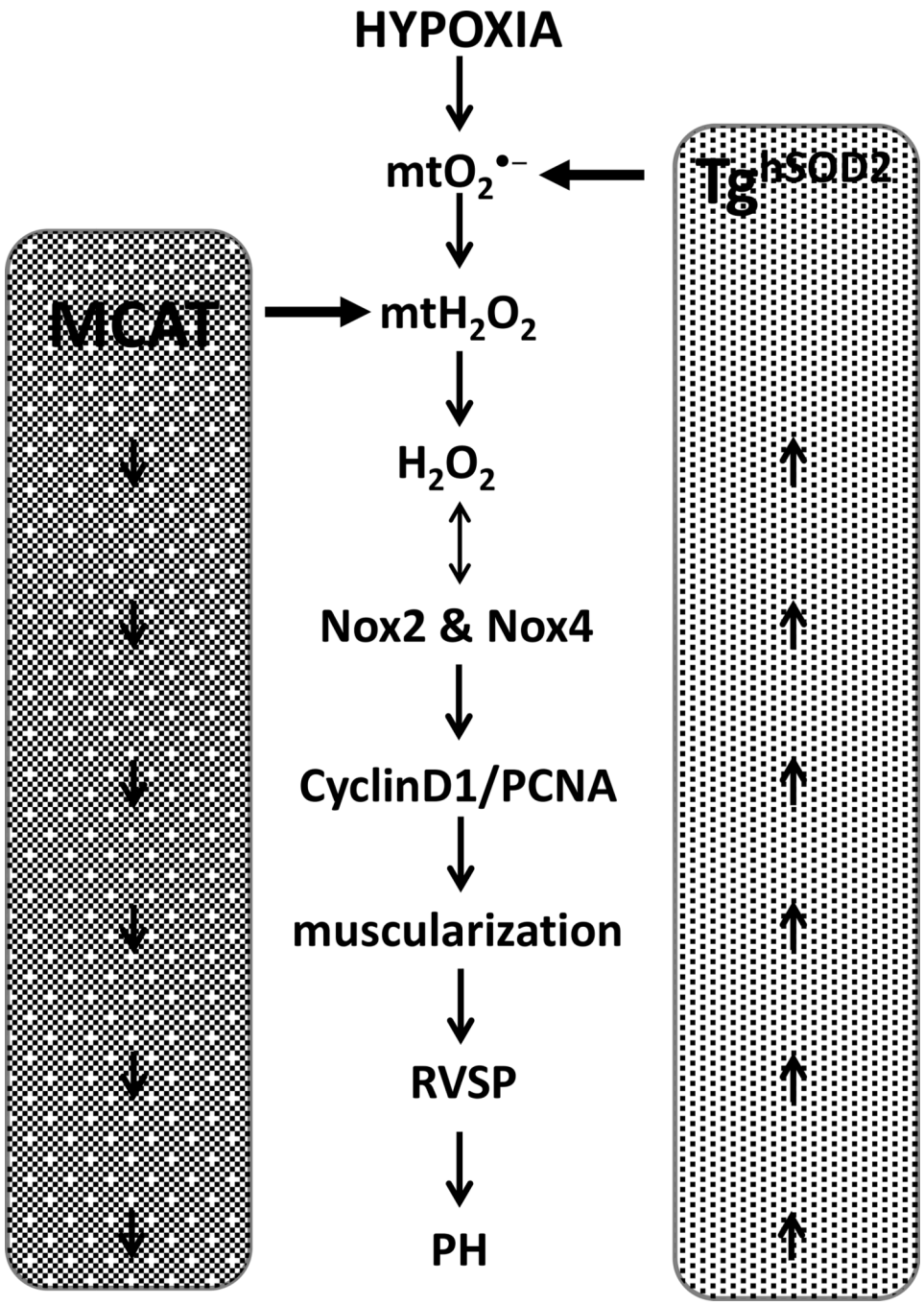

Figure 7. Schematic representation of the role of mitochondria ROS in the development of PH

Targeted attenuation of mtH_2O_2 with MCAT model (left side of schema) prevents hypoxia-induced PH molecular and physiological derangements. Conversely, targeted inhibition of $mtO_2^{\bullet-}$ (right side of schema) exacerbates hypoxia-induced derangements that contribute to PH pathogenesis.